CrossMark

ORIGINAL PAPER

Failure Mechanism and Acoustic Emission Characteristics of Rock Specimen with Edge Crack Under Uniaxial Compression

Yujing Jiang · Hengjie Luan ⓘ · Dong Wang · Changsheng Wang · Wei Han

Abstract There are many cracks in rock mass which have a significant influence on the stability of rock engineering. Most of current researches on the failure mechanism of cracked rock are mainly focused on the internal cracks. However, edge cracks around underground openings are common in many engineering fields. Understanding the failure mechanism of rock with edge cracks is essential to assess the stability of underground structures. Rock failure is closely related to the cracking processes and acoustic emission characteristics is deemed as an effective means of monitoring the cracking processes of rock. In this study, a series of numerical simulations utilizing particle flow software PFC2D were performed to investigate the influence of the length and position of edge crack on the failure mechanism and acoustic emission characteristics of rock specimens with edge cracks under uniaxial compression. The results show that: the strength of specimens is sensitive to the change of crack length and position; the directions of crack propagation in each specimen is in good agreement, the different crack tip position and the specimen boundary lead to different failure modes; the influence of crack length on acoustic emission is greater than that of crack position.

Keywords Edge crack · Compression strength · Failure mechanism · Acoustic emission

Y. Jiang · H. Luan (✉) · D. Wang (✉) ·
C. Wang · W. Han
State Key Laboratory of Mining Disaster Prevention and Control Co-founded BY Shandong Province and the Ministry of Science and Technology, Shandong University of Science and Technology, Qingdao 266590, China
e-mail: luanjie0330@126.com

D. Wang
e-mail: wdwinter@163.com

Y. Jiang · H. Luan · D. Wang · C. Wang · W. Han
College of Mining and Safety Engineering, Shandong University of Science and Technology, Qingdao 266590, China

Y. Jiang · C. Wang
Graduate School of Engineering, Nagasaki University, Nagasaki 852-8521, Japan

1 Introduction

Rock mass is a discontinuous material composed of rock and a large number of fractures in the form of joints, cracks, fissures, etc. (Wang et al. 2017a, b; Cao et al. 2016a, b). Cracked rock mass, which affect the stability of geological engineering to a great extent, is the most common discontinuity encountered in large-scale geotechnical engineering, such as transportation, national defense, water conservancy and hydropower, and mining (Huang et al. 2017; Yang et al. 2014a, b). The phenomenon of geotechnical engineering failure has been common and caused huge economic losses, such as Malpasset Dam and Vaiont Landslide. Much

of engineering cases show that cracks propagation and coalescence under loads lead to a degradation in the mechanics properties of rock, this will result in rock mass failure (Cheng et al. 2016; Zhang et al. 2015). Hence, the instability of cracked rock mass has been an important research topic in the field of rock mechanics and rock engineering (Liu et al. 2017a, b; Cao et al. 2016a, b). In order to understand the mechanism of cracked rock specimens under uniaxial loading, numerous experiments, numerical methods and theoretical efforts were devoted to investigating the macro mechanical behavior of cracked rock in the past decades (Wang et al. 2014, 2016; Zhou et al. 2014, 2015). However, previous work on the failure mechanism of cracked rock was mainly focused on the internal crack (Liu et al. 2016, 2017a, b; Zhang and Wong 2011; Yang et al. 2014a, b). Edge cracks, which are around the edge of underground openings, are common in many engineering fields, such as mining, tunneling, water conservancy and radioactive disposal facilities. Understanding the failure mechanism of rock with edge crack can contribute to prevention and control of geotechnical engineering disasters. At present, research production of edge crack propagation on theoretical analysis, mechanical test, numerical simulation and so on are few, and there are many shortages in the application of solving the field engineering problems. Therefore, the failure mechanism of rock with edge crack needs to be studied more deeply. The damage and rupture of the rock are accompanied by acoustic emission (AE), which can be used to monitor and predict the propagation and penetration of micro-cracks in the rock on a continuous, real-time, and effective basis (Wen et al. 2016; 2017). The study of rock failure modes and acoustic emission characteristics will help to further understand the failure mechanism of rock. This technology appeared in the twentieth century and was already used in the rock mechanics community in the 70s (Hardy 1972; Lockner and Byerlee 1977). However, the research on acoustic emission characteristics of rock specimen with edge crack under uniaxial compression is relatively few. In this study, a series of numerical simulations utilizing particle flow software PFC2D were performed to investigate the influence of the length and position of edge crack on the failure mechanism and acoustic emission characteristics of rock specimen with edge crack under uniaxial compression.
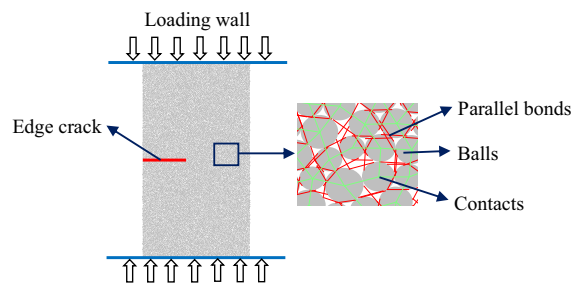
2 Numerical Simulation Method

2.1 Particle Flow Code

The particle flow code program is a numerical simulation technique based on the Cundall discrete element method; it considers the basic mechanical properties of the medium from the point of view of the basic particle structure of the medium and considers that the basic characteristics of the given medium under different stress conditions depend mainly on the change in contact state between particles (Cundall and Strack 1979). It has been widely used in the field of geotechnical engineering and used to simulate continuous and discontinuous material macro-meso mechanical behavior because the crack initiation and propagation in the medium can be quantitatively studied at the mesoscopic level (Cundall 1971). The parallel bond PFC model has unique advantages in simulating the meso damage of rock specimens. In the role of external compression loading, the internal particles are extruded and lead to relative displacement and continuous rotation, along with the continuous initiation and propagation of the tension crack and shear crack. PFC can use the FISH to realize real-time monitoring of the number of cracks.

2.2 Numerical Models of Rock Specimens with Different Edge Crack

The numerical models of rock specimens with edge crack are generated by PFC2D software, as shown in Fig. 1. The width and height of numerical models are 100 mm and 200 mm respectively. In PFC, the constitutive relation of the material is simulated by a contact constitutive model. The microscopic parameters are very important for numerical results. Usually,

Fig. 1 Numerical models of rock specimens with different edge cracks

the numerical simulation results are compared against the results of laboratory tests or in situ field tests. The microscopic parameters are adjusted repeatedly by trial and error method until they satisfy the requirement of simulation analysis. The microscopic parameters used are shown in Table 1 (Zhang and Wong 2014). Paper (Wang et al. 2017a, b) has compared the numerical results with experimental results and proved that these parameters are suitable in PFC2D to simulate rock material. The crack is represented by deleting the particles contained in the edge crack. The plane stress condition was assumed and the same loading speed (by moving the top wall) of 0.01 mm/s was adopted.

To quantitatively investigate failure mechanism and acoustic emission characteristics of rock specimens with edge crack under uniaxial compression, a series of numerical simulations utilizing particle flow software PFC2D were performed, in which, specimens with different edge crack lengths and positions were adopted. In the first set of numerical models, the edge cracks were located at the left of the specimen, the middle height, and their length are 0, 10, 20, 30, 40 and 50 mm, respectively, as shown in Fig. 2. In the second set of specimens, the edge cracks are located on the left and their length is 30 mm, the positions in the height direction are $+60$, $+30$, 0, -30 and -60 mm, respectively, as shown in Fig. 3.

2.3 PFC Simulation for Acoustic Emission

In the role of external compression loading, the internal particles of specimen are extruded and lead
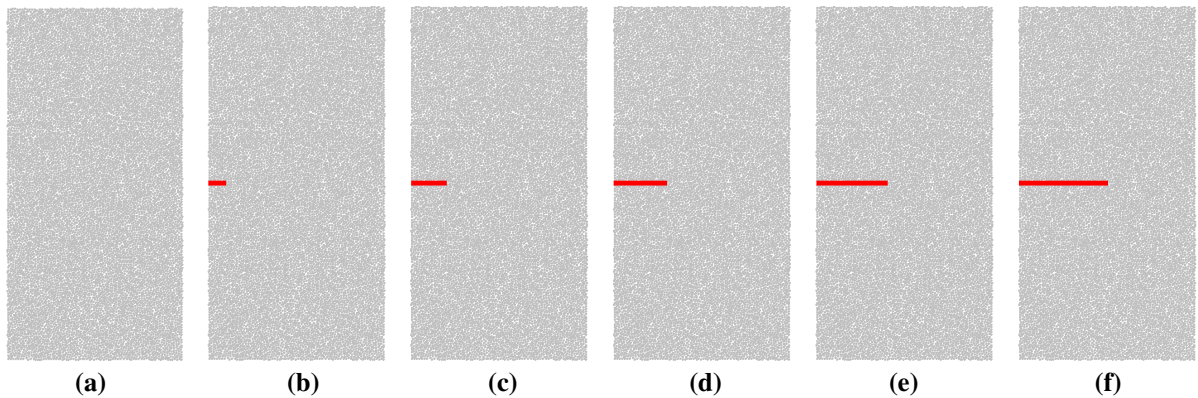
to relative displacement and continuous rotation. The force and moment of bonding between particles are increased and when the strength exceeds its strength, the bond will break, resulting in a tensile crack or a shear crack, and the number of parallel bonds will decrease. The appearance of the crack indicates that the specimen is damaged. During the extension of micro-cracks, the expended energy will be quickly released in the form of acoustic waves, which is referred to as acoustic emission. The parallel bond PFC model has unique advantages in simulating the meso damage of rock specimens. PFC can use the FISH to realize real-time monitoring of the number of cracks. In this way, acoustic emission characteristics can be studied.

3 Result Analysis and Discussion

3.1 Numerical Specimens with Different Edge Crack Lengths

3.1.1 Strength Characteristics

The stress–strain curves and peak strengths of numerical specimens with different edge crack lengths are, respectively, presented in Figs. 4 and 5. It can be seen that the slopes of the stress–strain curves decrease with the increase of the edge crack lengths in the elastic compaction stage, and the longer the crack is, the shorter the elastic compression stage. The compressive space of the specimens appears due to the existence of the crack, which leads to the reduction of the elastic modulus of the specimens. Moreover, with the increase of the crack length, the stress strain curves fluctuate several times near the peak stress position. This is due to the propagation of the crack from the tip to the different directions in many times, the longer the crack is, the more obvious the fluctuation is and the more times the fluctuation will occur. With the crack length increases from 0 to 50 mm, the peak strengths of numerical specimens are 60.83, 58.00, 53.37, 51.83, 50.14, 46.8 MPa respectively, the peak strength of numerical specimens decreases gradually. When the crack length increases from 0 to 50 mm, the decrease rate of the peak strengths of numerical specimens is 23.10%. This shows that the strength of specimens is sensitive to the change of the crack length. When the crack length is from 0 to

Table 1 Micro-parameters of rock specimen

Micro-parameters	Value
Minimum particle diameter (mm)	0.5
Particle diameter ratio	1.66
Density (kg/m^3)	1830
Contact modulus of the particle (GPa)	3.95
Ball stiffness ratio	1.0
Coefficient of friction	0.5
Parallel bond normal strength (MPa)	24.5 ± 6.5
Parallel bond shear strength (MPa)	24.5 ± 6.5
Parallel bond Deformation modulus (GPa)	3.95
Parallel-bond stiffness ratio	1.5

Fig. 2 Rock specimens with different edge crack lengths. **a** 0 mm, **b** 10 mm, **c** 20 mm, **d** 30 mm, **e** 40 mm, **f** 50 mm
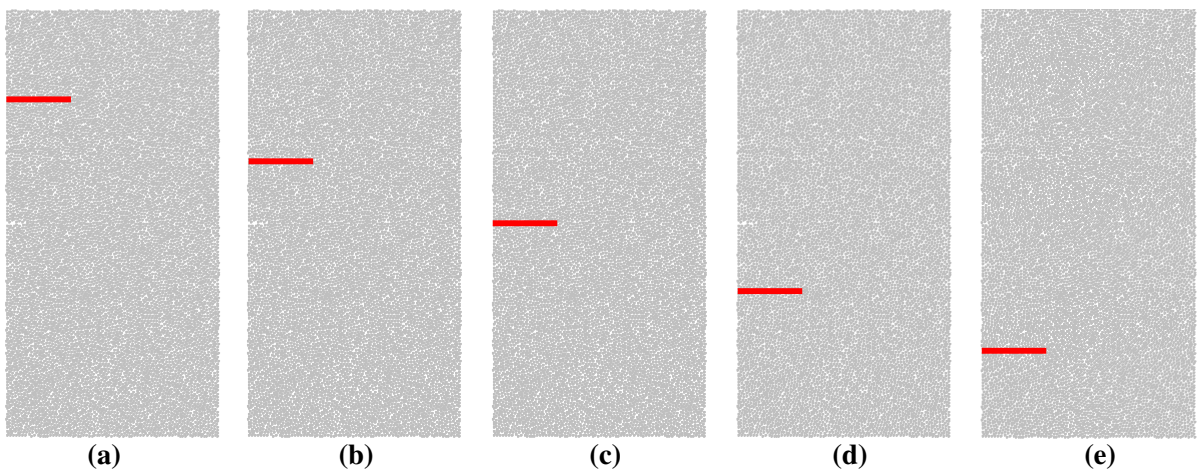
Fig. 3 Rock specimens with different edge crack positions. **a** + 60 mm, **b** + 30 mm, **c** 0 mm, **d** − 30 mm, **e** − 60 mm
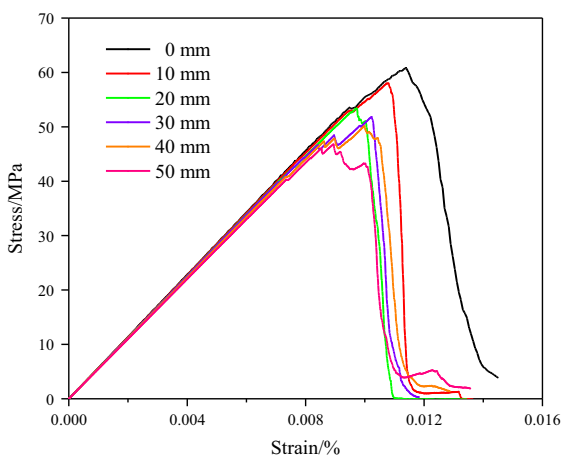
**Fig. 4** Stress–strain curves of numerical specimens with different crack lengths

20 mm, the reduction rate of peak strength is greater than that from 20 mm to 50 mm.

3.1.2 Failure Mechanism

Figure 6 depicts the failure modes of specimens with different edge crack lengths, blue represents the tension crack, and red represents the shear crack. In Fig. 6, it can be seen that the failure modes of numerical specimens with different edge crack lengths are different. A large number of tensile cracks were produced during the specimen failure process. Tension cracks are mainly caused by severe extrusion between particles, meeting the compression-induced tension cracks mechanism, as shown in Fig. 7 (Liu et al. 2016). Then, the specimen with a crack length of

30 mm is taken as an example to describe the failure process of the specimen. It can be seen from Fig. 8, as the compression degree between particles increases, the cracks began to extend from the tip of the edge crack to the bottom of the specimen in the direction of 60° (C-1). When the crack extended to the bottom of the specimen, the crack began to propagate along a symmetrical direction to the right edge (C-2). Then, an asymmetric V type failure mode was formed and the extent of the asymmetry is related to the length of the crack. However, when the crack length is 40 mm and 50 mm, a main crack appeared in the upper left corner of the specimen (C-3). By comparing the cracks in each specimen, it can be seen that the directions of the cracks (C-1, C-2 and C-3) in each specimen are in
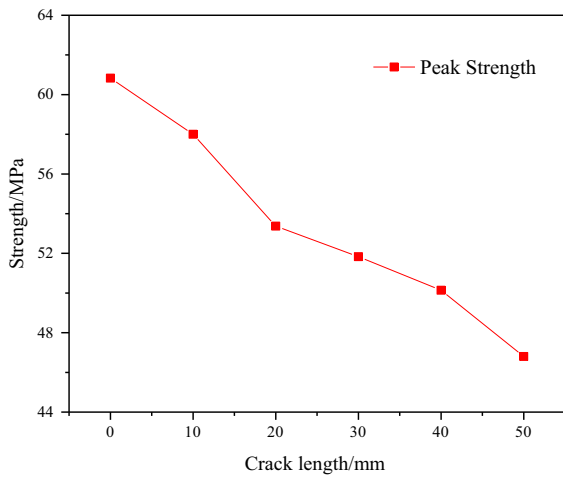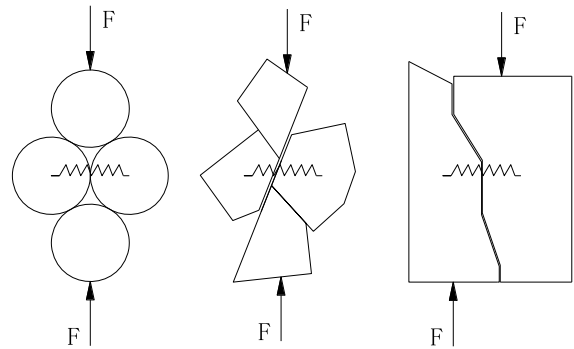
good agreement. However, the crack tip position and the specimen boundary play a limiting role in the development of the crack, so the specimens have different failure modes.
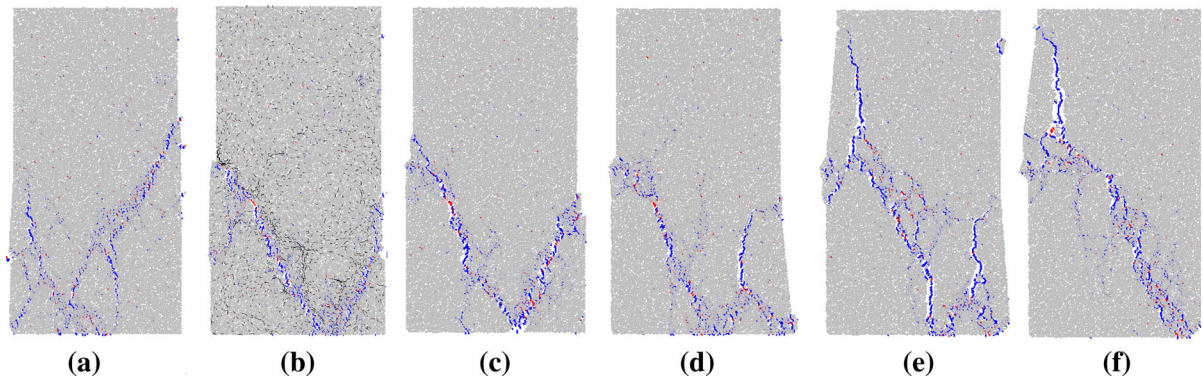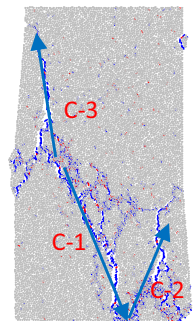
3.1.3 Acoustic Emission Characteristics

Figures 9 and 10 show the stress–strain–AE characteristic curves and strain-AE characteristic contrast

**Fig. 7** Illustration of compression-induced tension

Fig. 8 Crack propagation path

Fig. 5 Peak strengths of numerical specimens with different crack lengths

Fig. 6 Failure modes of numerical specimens with different edge crack lengths. **a** 0 mm, **b** 10 mm, **c** 20 mm, **d** 30 mm, **e** 40 mm, **f** 50 mm
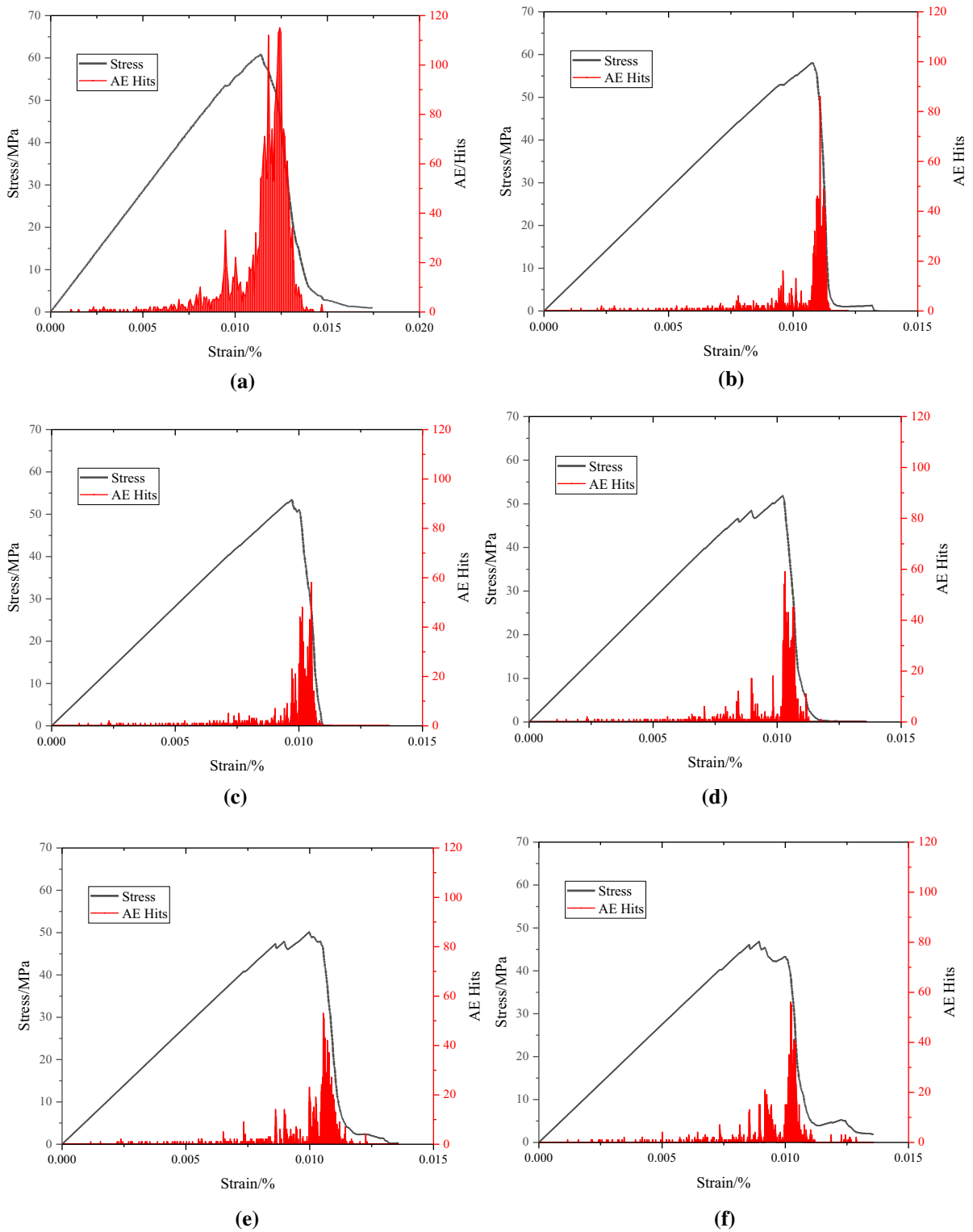
Fig. 9 Stress–strain–AE characteristic curves of numerical specimens with different crack lengths. **a** 0 mm, **b** 10 mm, **c** 20 mm, **d** 30 mm, **e** 40 mm, **f** 50 mm
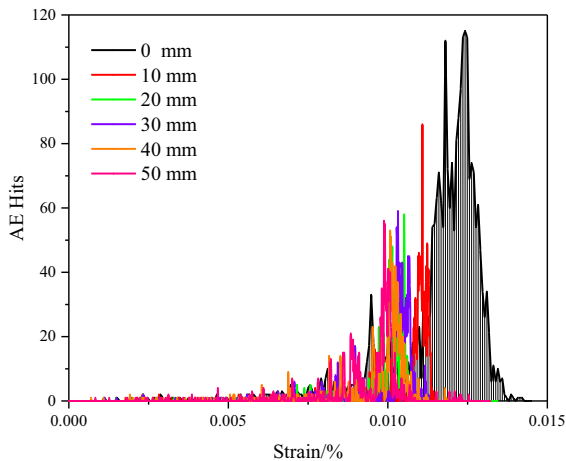
**Fig. 10** Strain–AE characteristic contrast curves of numerical specimens with different crack lengths

curves of numerical specimens with different edge crack lengths, respectively. It can be seen that the shapes of strain–AE characteristic curves are strongly consistent. When the strain is small, the acoustic emission hits strength and number are very little. Then, the acoustic emission intensity begins to increase gradually and reaches the maximum. Finally, the intensity drops sharply. However, when the strain exceeds 0.07%, the peak intensity of acoustic emission of the specimen and the strain position corresponding to the peak intensity of acoustic emission begin to have a greater difference. The acoustic emission intensity of the specimen without crack is the highest, the acoustic emission hits is 115 and the strain range with obvious emission phenomenon is also larger. The maximum acoustic emission intensity of specimens with crack length of 10 mm is 86, which decreases by 41.46% compared with the specimen without crack, and the strain range of the obvious emission decreases as well. The acoustic emission intensity of specimens with crack length ranging from 20 to 50 mm is 58, 59, 53 and 56 respectively, which is about 52.92% lower than that of the specimen without crack. However, the acoustic emission strength change of the specimens with crack length in this range is not obvious, and the acoustic emission characteristics are similar. When the specimen without crack, a large area of damage will occur first and the acoustic emission signal is much higher than that with crack, indicating that the existence of the initial crack causes the specimen to damage earlier along the weak part, and the damage

range is smaller. The acoustic emission signal has several small fluctuations before reaching its peak, resulting in several small peaks corresponding to fluctuations in stress peaks. The above phenomena indicate that when the crack is generated and the acoustic emission signal is produced, the damage is produced inside the specimen, resulting in the reduction of specimen strength.
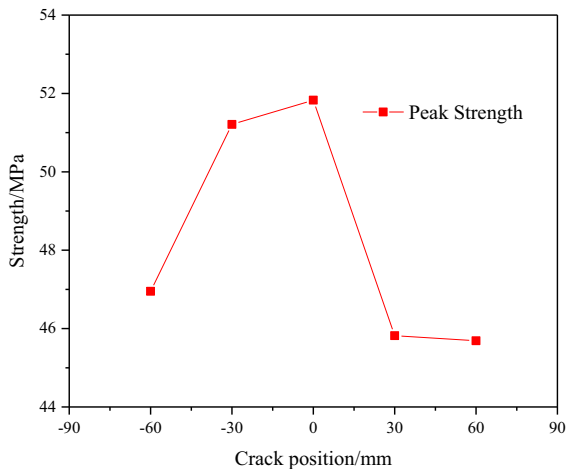
3.2 Numerical Specimens with Different Edge Crack Positions

3.2.1 Strength Characteristics

In Figs. 11 and 12, according to the stress–strain curves and peak strengths of numerical specimens with different edge crack positions, it can be seen that, in the elastic compression stage, the slope of the stress–strain curve is different. When the crack position is 0 mm, the curve slope is the largest, followed by − 30, + 30, + 60 and − 60 mm. The slope of the stress–strain curve decreases with the change of the position of the edge crack from the middle to the ends of specimen. The closer the crack is to the two ends, the shorter the elastic compression stage is, and the earlier the specimen enters the failure stage. This indicates that the constraints of the crack which near the ends is weakened, so it is easier to deform. The stress strain curve fluctuates several times near the peak stress position, this is due to the expansion of the crack from the tip to the different
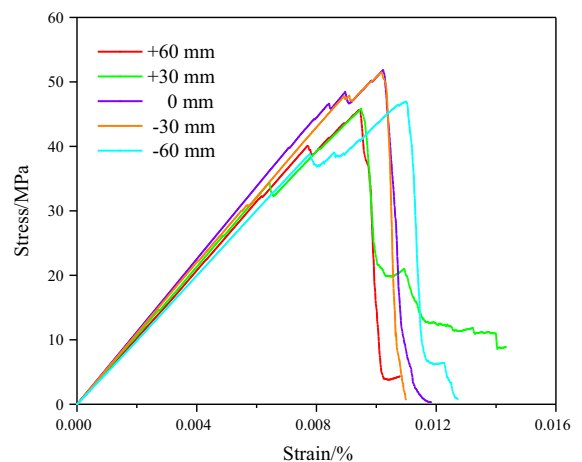
Fig. 11 Stress–strain curves of numerical specimens with different crack positions

Fig. 12 Peak strengths of numerical specimens with different crack positions

directions in many times. When the crack positions are + 60 mm, + 30 mm, 0 mm, − 30 mm and − 60 mm, the peak strength of numerical specimen is 45.69, 45.82, 51.83, 51.21 and 46.95 Mpa respectively. The crack position changes from middle to both ends, and the peak strength of the specimens decreases gradually, and the maximum reduction rate is 11.85%. This shows that the strength of specimens is sensitive to the change of crack position.

3.2.2 Failure Mechanism

Figure 13 depicts the fracture modes of numerical specimens with different edge crack positions. Blue represents the tension crack, and red represents the shear crack. In Fig. 13, it can be seen that the failure modes of numerical specimens with different edge crack position are distinctly different. When the crack positions are + 60 mm and + 30 mm, the cracks begin to extend from the tip of the edge crack to the top of the specimens in the direction of 60°, when the crack extends to the top of the specimen, the crack begins to propagate a symmetrical direction to the right edge. When the crack position is 0 mm, the cracks begin to extend from the tip of the edge crack to the bottom of the specimen in the direction of 60°. The crack begins to propagate in a symmetrical direction to the right edge when the crack extends to the bottom of the specimen. When the crack position is − 30 mm, the cracks begin to extend from the tip of the edge crack to the base of the specimen in the direction of 60°, then the specimen completely destroyed. When the crack position is − 60 mm, the cracks begin to extend from the tip of the edge crack to the base of the specimen in the direction of 60°, then the specimen is extended to the right side of the specimen in the 60° direction from the tip of the edge crack and the bottom of the specimen. In general, the failure modes of specimens are dominated by shear slip failure which has obvious directionality and is affected by the boundary of specimens. The final failure of the specimens is the result of the combined effect of the crack positions, the property of the specimens and the influence of the boundary of the specimens.
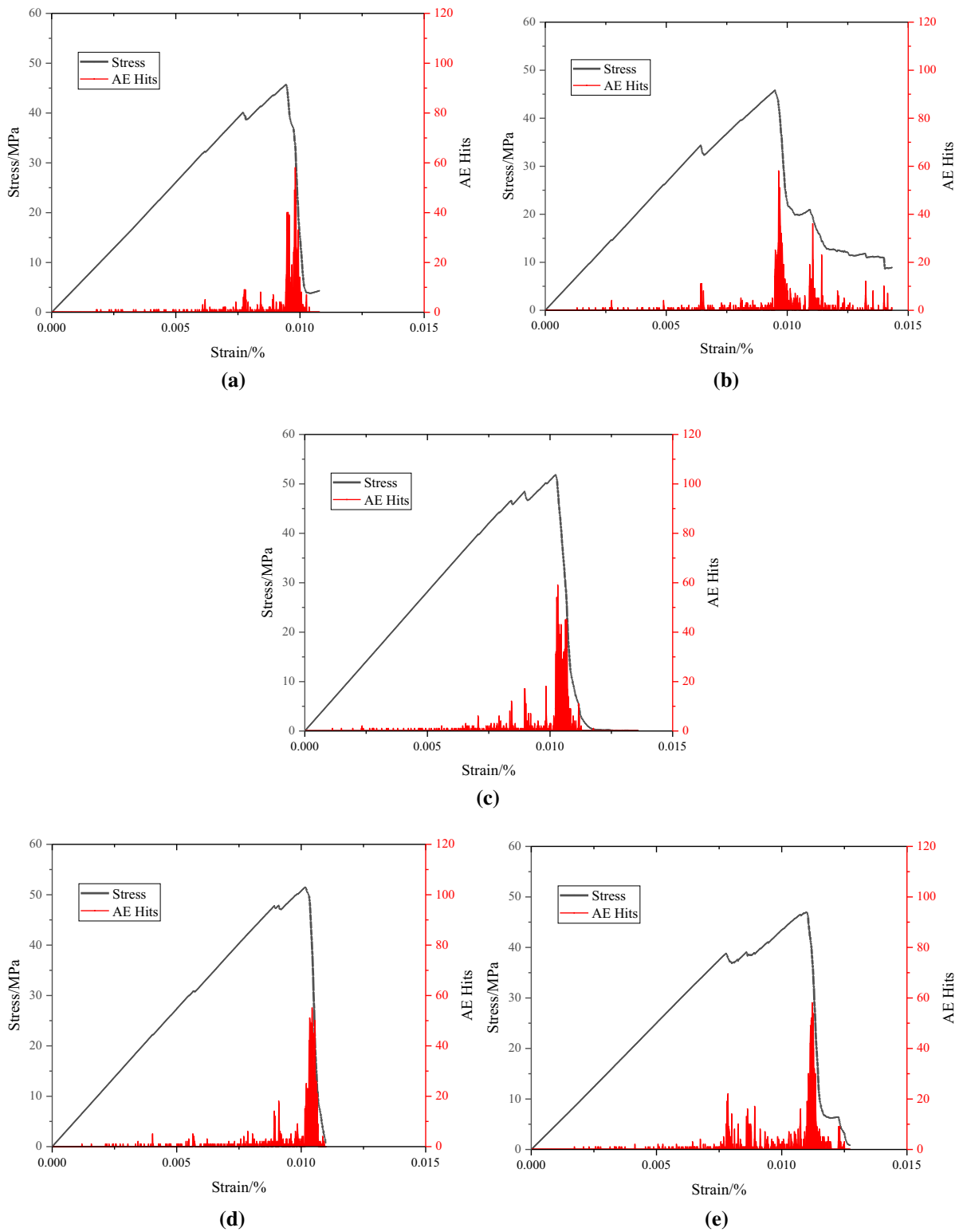
3.2.3 Acoustic Emission Characteristics

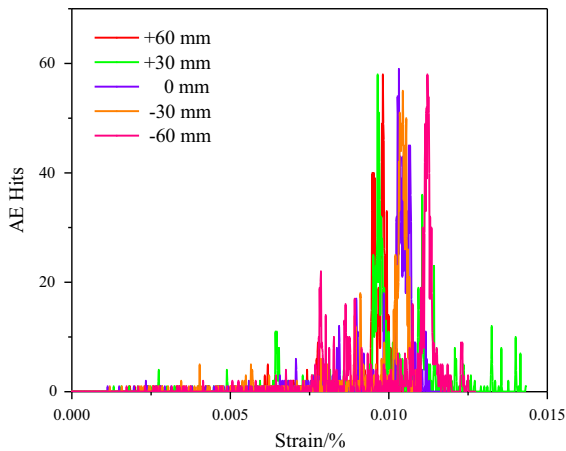Figures 14 and 15 show the stress–strain–AE characteristic curves and strain–AE characteristic contrast
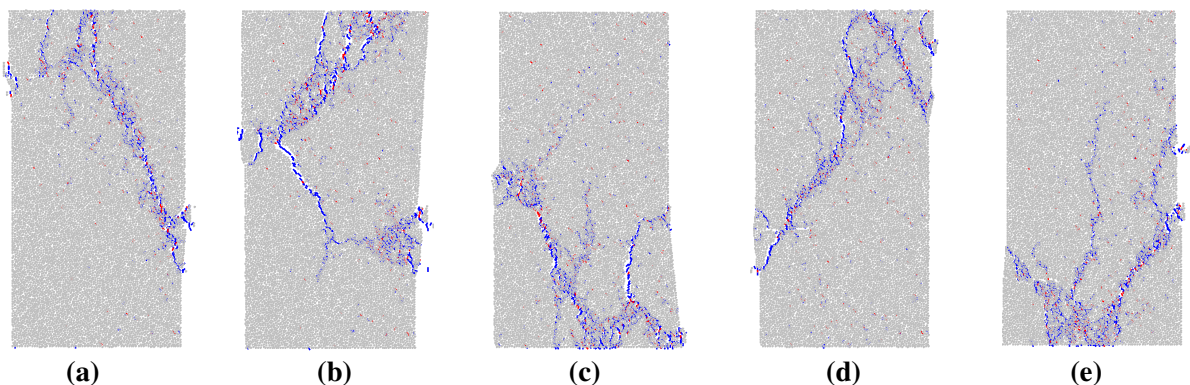
Fig. 13 Failure modes of numerical specimens with different edge crack positions. **a** + 60 mm, **b** + 30 mm, **c** 0 mm, **d** −30 mm, **e** −60 mm

Fig. 14 Stress–strain–AE characteristic curves of numerical specimens with different crack positions. **a** + 60 mm, **b** + 30 mm, **c** 0 mm, **d** −30 mm, **e** −60 mm

Fig. 15 Strain–AE characteristic curves of numerical specimens with different crack positions

curves of numerical specimens with different edge crack positions, respectively. It can be seen that when the crack positions are + 60 mm, + 30 mm, 0 mm, − 30 mm and − 60 mm, the peak intensities of acoustic emission of specimens are 58, 58, 59, 55 and 58 Mpa, respectively. The effect of crack position on the acoustic emission peak intensity is not obvious. However, the fluctuations of acoustic emission signals at are significantly different before and after the peak stage. When the crack positions are + 60 mm, 0 mm and − 30 mm, several small fluctuations occur mainly before the peak; when the crack position is + 30 mm, several small fluctuations appear before the peak, and a few large fluctuations occur after the peak; when the crack position is − 60 mm, a few large fluctuations appear before the peak. This phenomenon is related to the failure modes of the specimens. Each time a primary crack occurs, a stronger acoustic emission signal is emitted. In addition, the strain positions corresponding to the peak acoustic emission intensity are also different.

4 Conclusions

1. The slope of the stress–strain curve decreased with the increase of the length of edge crack in the elastic compaction stage, the longer the crack is, the shorter the elastic compression stage. The strength of specimens is sensitive to the change of the crack length.

2. The failure modes of numerical specimens with different edge crack lengths are different. An asymmetric V type failure mode was formed and the extent of the asymmetry is related to the length of the crack. The crack tip position and the specimen boundary play a limiting role in the development of the crack.

3. The acoustic emission intensity of the specimen without crack is the highest, the maximum acoustic emission intensity of specimens with crack length of 10 mm decreases by 41.46%. The acoustic emission intensity of specimens with crack length ranging from 20 to 50 mm is about 52.92% lower than that of the specimen without crack.

4. The closer the crack is to the two ends, the shorter the elastic compression stage is, and the earlier the specimen enters the failure stage. The crack position changes from middle to both ends, and the peak strength of the specimens decreases gradually.

5. The failure modes of numerical specimens with different edge crack positions are distinctly different. This is because the shear slip failure of specimen has obvious directionality and is affected by the boundary.

6. The effect of crack position on the acoustic emission intensity is not obvious. The strain positions corresponding to the peak acoustic emission intensity are different.

References

Cao R et al (2016a) An experimental and numerical study on mechanical behavior of ubiquitous-joint brittle rock-like specimens under uniaxial compression. Rock Mech Rock Eng 49(11):4319–4338

Cao R et al (2016b) Mechanical behavior of brittle rock-like specimens with pre-existing fissures under uniaxial loading: experimental studies and particle mechanics approach. Rock Mech Rock Eng 49(3):763–783

Cheng H et al (2016) The effects of crack openings on crack initiation, propagation and coalescence behavior in rock-

like materials under uniaxial compression. Rock Mech Rock Eng 49(9):3481–3494

Cundall PA (1971) A computer model for simulating progressive large scale movements in blocky system. In: Muller LED (ed) Proceedings of symposium of the international society of rock mechanics, vol 1. A. A. Balkema, Rotterdam, pp 8–12

Cundall PA, Strack ODL (1979) A discrete numerical method for granular assemblies. Geotechnique 29(1):47–65

Hardy HR (1972) Application of acoustic emission techniques to rock mechanics research. In: Liptai RG, Harris DO, Tatro CA (eds) Acoustic emission. ASTM International, Pennsylvania, pp 41–83

Huang Y et al (2017) Strength failure behavior and crack evolution mechanism of granite containing pre-existing non-coplanar holes: experimental study and particle flow modeling. Comput Geotech 88:182–198

Li S, Wang S, Wang ZY (2018) Microparameter estimation method of concrete micro-constitutive model based on brazilian test. J Shandong Univ Sci Technol (Nat Sci) 37(4):49–57

Liu T et al (2016) Mechanical behaviors and failure processes of precracked specimens under uniaxial compression: a perspective from microscopic displacement patterns. Tectonophysics 672–673:104–120

Liu T, Lin B, Yang W (2017a) Mechanical behavior and failure mechanism of pre-cracked specimen under uniaxial compression. Tectonophysics 712–713:330–343

Liu Y et al (2017b) Experimental investigation of the influence of joint geometric configurations on the mechanical properties of intermittent jointed rock models under cyclic uniaxial compression. Rock Mech Rock Eng 50(6):1453–1471

Lockner D, Byerlee J (1977) Acoustic emission and creep in rock at high confining pressure and differential stress. Bull Seismol Soc Am 67(2):247–258

Wang SY et al (2014) Numerical study of failure behaviour of pre-cracked rock specimens under conventional triaxial compression. Int J Solids Struct 51(5):1132–1148

Wang Y, Zhou X, Xu X (2016) Numerical simulation of propagation and coalescence of flaws in rock materials under compressive loads using the extended non-ordinary state-based peridynamics. Eng Fract Mech 163:248–273

Wang G et al (2017a) Macro–micro failure mechanisms and damage modeling of a bolted rock joint. Adv Mater Sci Eng 2017:1–15

Wang X, Jiang Y, Li B (2017b) Experimental and numerical study on crack propagation and deformation around underground opening in jointed rock masses. Geosci J 21(2):291–304

Wen ZJ, Wang X, Li QH et al (2016) Simulation analysis on the strength and acoustic emission characteristics of jointed rock mass. Tech Gaz 23(5):1277–1284

Wen Z et al (2017) Size effect on acoustic emission characteristics of coal-rock damage evolution. Adv Mater Sci Eng 2017:1–8

Yang S et al (2014a) Discrete element modeling on fracture coalescence behavior of red sandstone containing two unparallel fissures under uniaxial compression. Eng Geol 178:28–48

Yang S, Jing H, Xu T (2014b) Mechanical behavior and failure analysis of brittle sandstone specimens containing combined flaws under uniaxial compression. J Cent South Univ 21(5):2059–2073

Zhang M (2018) Roadway support technology in goaf of ultra-close distance coal seams. J Shandong Univ Sci Technol (Nat Sci) 37(4):35–41

Zhang X, Wong LNY (2011) Cracking processes in rock-like material containing a single flaw under uniaxial compression: a numerical study based on parallel bonded-particle model approach. Rock Mech Rock Eng 45(5):711–737

Zhang X, Wong LNY (2014) Displacement field analysis for cracking processes in bonded-particle model. Bull Eng Geol Environ 73(1):13–21

Zhang X et al (2015) Crack coalescence between two non-parallel flaws in rock-like material under uniaxial compression. Eng Geol 199:74–90

Zhao LQ, Feng JW (2018) Interrelationship study between rock mechanical stratigraphy and structural fracture development. J Shandong Univ Sci Technol (Nat Sci) 37(1):35–46

Zhou XP, Cheng H, Feng YF (2014) An experimental study of crack coalescence behaviour in rock-like materials containing multiple flaws under uniaxial compression. Rock Mech Rock Eng 47(6):1961–1986

Zhou XP, Bi J, Qian QH (2015) Numerical simulation of crack growth and coalescence in rock-like materials containing multiple pre-existing flaws. Rock Mech Rock Eng 48(3):1097–1114